



Soft Computing Models for Crop Acreage Estimation using Multi-sensory Satellite Images

Anand N Khobragade*Scholar, CSE, GHRCE, Nagpur,
Maharashtra, India**Mukesh M Raghuvanshi**Professor, CTD, YCCE, Nagpur,
Maharashtra, India**Latesh Malik**HOD, CSE, GHRCE, Nagpur,
Maharashtra, India

Abstract— This Now a days satellite images are used for broad spectrum of applications that leverages in decision making of government departments. Multi-spectral remote sensing images are widely used for large scale classification problems. However, hyperspectral satellite images are used in application like detection of minerals, detection of water bodies, vegetation analysis etc. The pre-processing of satellite image is done on ENVI, which is a revolutionary image processing system for the visualization, analysis, and presentation of all types of digital imagery, especially hyper-spectral images. Flaash module is used to remove atmospheric interference, whereas spectral hour glass wizard in ENVI which is effectively used for selections of best bands suitable for vegetation analysis, rather crop classification problems using satellite images. Researchers have used Minimum Noise Fraction (MNF) and Pixel Purity Index (PPI) methods for cleaning of multi-sensory satellite images that may be prone to errors. Support Vector Machine (SVM) is the best hybrid learning model for classifying hyper-spectral images in context with agricultural applications. Crop acreage estimation is a critical and foremost step towards effective agricultural monitoring systems. The ability to identify crop type makes it possible to estimate the agricultural area allocated under crop and hence compute relevant statistics providing essential information for crop control of area-based subsidies. The capabilities of microwave remote sensing images (e.g. SAR) for discriminating crop type have been explored not only using open source softwares like PolSAR, SARscape, TARANG, but proprietary softwares viz. ENVI and ERDAS Imagine too. The studies have been carried out upon various microwave data like CEOs, RISAT, RADARSAT, ENVISat, ASAR, or Polarimetric SAR with multi-temporal and multi polarized datasets. Multi-sensory satellite images are thus proves to be vital source for classifying or crop acreage and production analysis problems.

Keywords— soft computing; remote sensing, SVM, multi-spectral, hyper-spectral, microwave, RISAT, SAR, ENVI

I. INTRODUCTION

The Remotely sensed data is an ideal source for mapping land features at a variety of spatial and temporal scales. Due to its multi-spectral nature and repetitive coverage, remote sensing data is the most suitable for rapid assessment of land use and land covers. By sampling the natural environment at regular intervals of time, a remote sensing sensor provides a continuous data stream of the earth surface, in the form of radiance information. Consequently, a Remote Sensing technology has potential in estimating area of specific land features at Regional/Command/District/Taluka/Village level due to its multi-spatial and multi-temporal nature[2][22].

For this reason, Ministry of Agriculture and Cooperation, Government of India (GOI) initiated project named Forecasting of Agriculture outputs through Satellite, Agrometeorology and Land based observations, which will make extensive use of state of the art remote sensing and GIS technologies for achieving mandate of central government. Department of Space (DOS) executes this project in participation with State Remote Sensing Applications Centers and State Agriculture Department.[2]. Crop production forecasting of major crops in the country namely rice, cotton, sugarcane, mustard, groundnut, etc. can be completed using multi-date single sensor remote sensing data for estimating specific crop[18], for example, RADARSAT data used for rice whereas ASTER & RESOURCESAT data used for cotton and sugarcane.

A national level project on kharif rice identification and acreage estimation is being carried out successfully for several states in India. Though the main growing season is predominantly winter but the uncertainty of getting cloud free data during the season has resulted in the use of microwave data. A feasibility study was taken up for early forecasting of the rabi rice area using microwave data. Hierarchical decision rule classification technique was used for the identification of the different land cover classes. The increase or decrease in the SAR backscatter due to progress in the crop phenology or due to delayed sowing respectively forms the basis for identifying the rice areas. The studies emphasizes upon the synergistic use of SAR and optical data for delineating the rabi rice areas which is of immense use in giving an early forecast on crops[23] [31].

In mathematics, 'Hyper-' indicates 4 or more dimensions. In remote sensing, the term in 'hyperspectral', indicates lots of bands. Some hyperspectral sensors, for example, have more than 200 bands. Although most hyperspectral sensors measure hundreds of wavelengths, it is not only the number of measured wavelengths that defines a sensor as hyperspectral, but also the narrowness and contiguous nature of the measurements. For example, a sensor that measures only 10 bands may be considered hyperspectral if those bands are contiguous and narrow. If a sensor measures 20

wavelength bands that are, say, 100 nm wide, or that are separated by non-measured wavelength ranges, the sensor would no longer be considered hyperspectral. Therefore, in order to be considered hyperspectral, three conditions should be satisfied – multiple bands, high spectral resolution (i.e. narrowness of each band), and contiguity of bands.

II. METHODOLOGY

A. Multi-spectral Image Classification

Multispectral images are acquired by means of remote sensing radiometers or sensors. Dividing the spectrum into many bands, multispectral is the opposite of panchromatic, which records only the total intensity of radiation falling on each pixel. Usually, satellite images captured in three or more channels. Each one used for acquiring single digital image in a small band of visible spectra, ranging from 0.7 μm to 0.4 μm, called red-green-blue (RGB) region, and going to infrared wavelengths of 0.7 μm to 10 or more μm. Remote Sensing Images are considered as most complex in nature as regards to image classification[1][7].

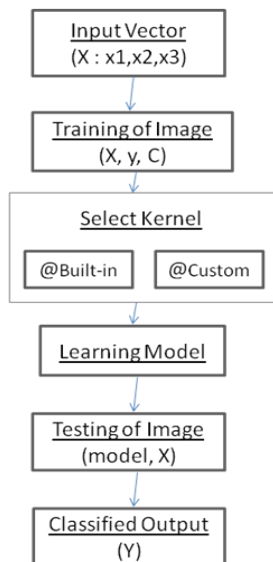


Fig.1 Flow Diagram for Multi-spectral Image Classification Process

The multispectral data uses minimum number of bands. multispectral data sets are usually composed of about 5 to 10 bands of relatively large bandwidths (70-400 nm). Entire cycle of image classification is to be adopted for evaluating kernel effect on SVM performance. Initially, input vector is created from multi-spectral satellite images. Feature vector is applied and again it must be exported to .CSV file or any compatible format commensurate with desired software, may be even geotiff image sometimes. Input vectors are labels for known samples so as to train our SVM model. The important step is to make appropriate choice of kernel functions, which significantly varies with the nature of application or complexity of classification problem.

B. Hyperspectral satellite Image Classification

The nature of remote sensing requires that solar radiation pass through the atmosphere before it is collected by the instrument. Because of this, remotely sensed images include information about the atmosphere and the earth’s surface. For those interested in quantitative analysis of surface reflectance, removing the influence of the atmosphere is a critical pre-processing step. Here Flaash module[11] is used to remove atmospheric interference. spectral hour glass wizard is the module in ENVI which is run to get end members spectra by removing bad bands from the reflectance data set. Bad bands are the bands containing noise. Minimum noise fraction step within this wizard uses two principle component to calculate Eigen values to plot good MNF bands. Pixel purity index uses iteration method to find extreme pixels from the image. n-D visualizer creates region of interest files to input to SVM. Finally the Support vector machine is applied on the ROI files to perform classification[12].

B.1 Atmospheric Correction Methods

Atmospheric correction is a major issue in visible or near-infrared remote sensing because the presence of the atmosphere always influences the radiation from the ground to the sensor. To compensate for atmospheric effects, properties such as the amount of water vapour, distribution of aerosols, and scene visibility must be known. Because direct measurements of these atmospheric properties are rarely available, there are techniques that infer them from their imprint on hyperspectral radiance data[9]. These properties are then used to constrain highly accurate models of atmospheric radiation transfer to produce an estimate of the true surface reflectance.

ENVI’s Fast Line-of-sight Atmospheric Analysis of Spectral Hypercube (FLAASH) module[11] is a first-principles atmospheric correction modeling tool for retrieving spectral reflectance from hyperspectral radiance images. FLAASH starts from a standard equation for spectral radiance at a sensor pixel, L, that applies to the solar wavelength range (thermal emission is neglected) and flat, Lambertian materials or their equivalents. The equation is as follows:

$$L = \left(\frac{A\rho}{1-\rho_e S} \right) + \left(\frac{B\rho_e}{1-\rho_e S} \right) + L_a \quad \text{where;}$$

- ρ - is the pixel surface reflectance
- ρ_e - is an average surface reflectance for the pixel and a surrounding region
- S - is the spherical albedo of the atmosphere
- $L\alpha$ - is the radiance back scattered by the atmosphere
- A & B - are coefficients that depend on atmospheric and geometric conditions but not on the surface.

Each of these variables depends on the spectral channel; the wavelength index has been omitted for simplicity. The first term in given equation corresponds to radiance that is reflected from the surface and travels directly into the sensor, while the second term corresponds to radiance from the surface that is scattered by the atmosphere into the sensor.

B.2 Spectral Hourglass Wizards

Following is the methodology applied in Hourglass wizard for hyperspectral satellite image classification.

Operational Hyperspectral Processing

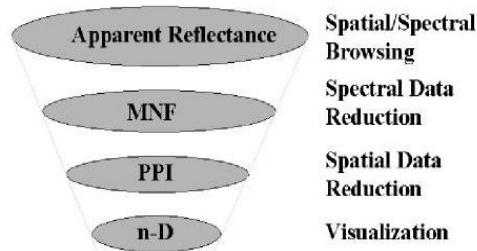


Fig.2 Methodology applied in Hourglass wizard

This Procedure includes the generation of Minimum Noise Fraction-Images (MNF) for data dimensionality estimation and reduction by decorrelating the useful information and separating noise (Green et al. 1988), Pixel Purity Index-Mapping (PPI) for the determination of the purest pixels in an image (as potential endmembers) utilizing the (uncorrelated) MNF-images and finally the extraction of endmembers (referred to as n-D-endmembers in the following) utilizing the n-Dimensional-Visualizer tool (n-D-Vis). The extracted endmembers were then compared to known spectra from spectral libraries for identification.

B.2.1 MNF Transformation

The Minimum Noise Fraction (MNF) transform is used to determine the inherent dimensionality of image data, to segregate and equalize the noise in the data, and to reduce the computational requirements for subsequent processing. The MNF transform uses two cascaded Principal components (PC) transformations. The first transformation, based on an estimated noise covariance matrix, decorrelates and rescales the noise in the data. This results in transformed data in which the noise has unit variance and no band-to-band correlations. The second transform is a standard Principal Components transformation of the noise-whitened data. The resulting bands of the MNF transformed data are ranked with the largest amount of variance in the first few bands and decreasing data variance with increasing band number until only noise and no coherent image remains.

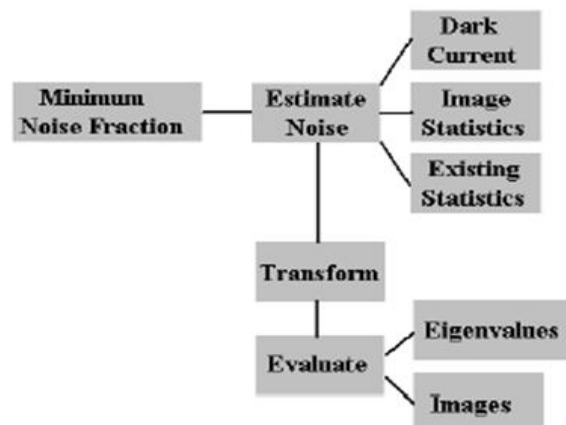


Fig.3 Minimum Noise Fraction model

B.2.2 Pixel Purity Index

The Pixel Purity Index (PPI) is used to find the most "spectrally pure," or extreme, pixels in multispectral and hyperspectral data. The most spectrally pure pixels typically correspond to mixing endmembers. The PPI is computed by repeatedly projecting n-dimensional scatter plots onto a random unit vector. The extreme pixels in each projection are recorded and the total number of times each pixel is marked as extreme is noted. The threshold value is used to define how many pixels are marked as extreme at the ends of the projected vector. The threshold value should be approximately 2-3 times the noise level in the data (which is 1 when using MNF transformed data). Larger thresholds cause the PPI to find more extreme pixels but they are less likely to be "pure" endmembers.

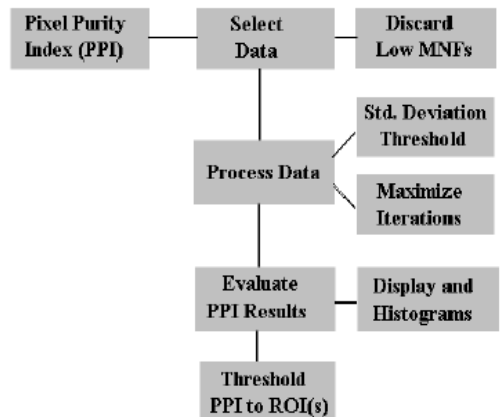


Fig.4 Pixel Purity Index (PPI) Model

B.2.3 n-D Visualizer

ENVI's n-Dimensional Visualizer provides an interactive tool for finding endmembers by locating and clustering the purest pixels in n-dimensional space. Spectra can be thought of as points in an n-dimensional scatter plot, where "n" is the number of MNF bands or dimensions. The coordinates of each point in n-space consist of "n" values that are simply the spectral radiance or reflectance values in each band for a given pixel.

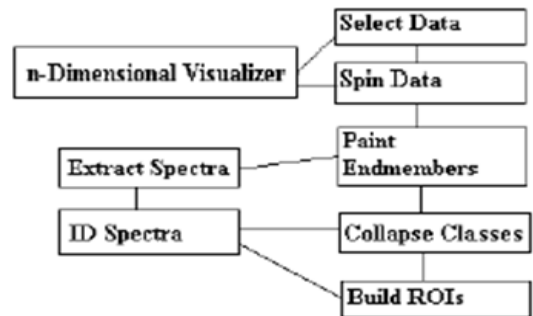


Fig.5 n-D Visualizer Process Flow

C. Microwave Satellite Image Classification

In a running system of crop area monitoring in large scale using remote sensing (RS), it is necessary to be timely, economical, reliable, and the most important comprehensive and accurate. In the monitoring system, the higher spatial resolution images gets high accuracy, but heavy workload and high cost, while the lower ones, gets low cost, high temporal resolution, and low identification accuracy[8].

Hence, the combination of different type of images is helpful to improve the identification accuracy of crop and realize operational crop monitoring in large scale. The research, based on the agricultural area estimation of Indian RISAT images, proposes the crop area identification method by processing the speckle noise which inherently exists in and degrades the quality of the active radar and SAR images [21].Reduction of speckle noise is one of the most important processes to increase the quality of radar coherent images[6].

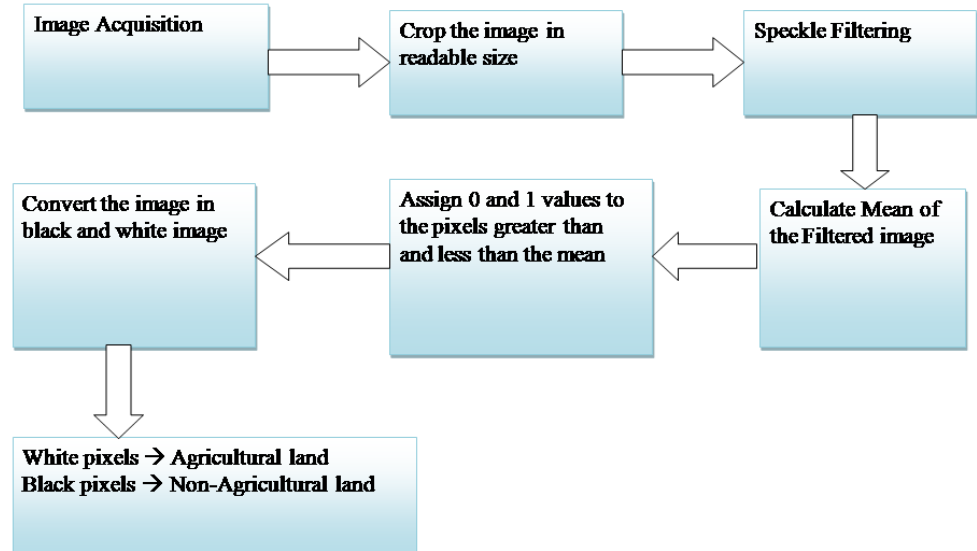


Fig.6 Process Flow for Diagram for Microwave Image Classification

C.1 Speckle Noise Reduction

Radar images are formed by coherent interaction of the transmitted microwave with the targets. Speckle noise which arises from coherent summation of the signals scattered from ground distributed randomly within each pixel[5]. Speckle, a form of multiplicative noise, occurs when a sound wave pulse randomly interferes with the small particles or objects on a scale comparable to the sound wavelength. Speckle, having a granular pattern, is the inherent property of ultrasound image and SAR (Synthetic Aperture Radar) image. Speckle noise can be reduced by multi-look processing or spatial filtering [30].

The ideal speckle reduction method preserves radiometric information, the edges between different areas and spatial signal variability, i.e., textural information. The spatial filters are categorized into two different groups, i.e., non-adaptive and adaptive. Non-adaptive filters take the parameters of the whole image signal into consideration and leave out the local properties of the terrain backscatter or the nature of the sensor, not appropriate for non-stationary scene signal. Adaptive filters accommodate changes in local properties of the terrain backscatter as well as the nature of the sensor. [5] Adaptive filters reduce speckles while preserving the edges (sharp contrast variation). Adaptive filter varies the contrast stretch for each pixel depending upon the Digital Number (DN) values in the surrounding moving kernel.

C.2 Quality Assessment Parameters

Important quality assurance parameters are Mean and Standard Deviation of satellite images. The mean is the arithmetic average of all the pixels grey values in the image;

$$\bar{Z} = \frac{\sum_{i=1}^M \sum_{j=1}^N Z(x_i)}{M \times N}$$

The standard deviation reflects the image’s gray scale distribution. A larger SD value indicates that the image contains more information; its contrast is more obvious.

$$\sigma = \sqrt{\frac{\sum_{i=1}^M \sum_{j=1}^N (Z(x_i, y_j))^2}{M \times N}}$$

The standard deviation gives information about the spread of the histogram. The change in the standard deviation of the distribution is considered in addition to the shift in the mean. A combination of these two metrics quantifies the changes in the shape of the histogram of each band.

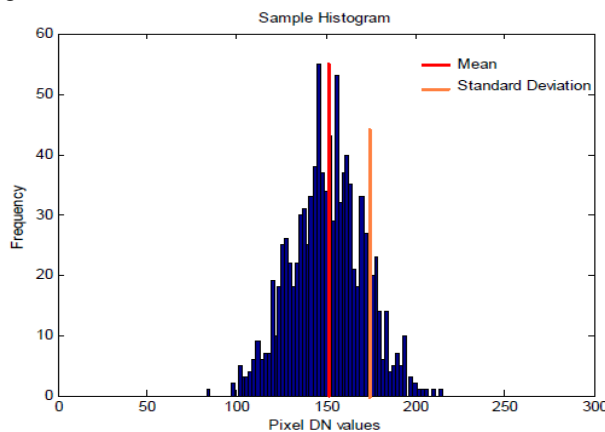


Fig.7 Histogram showing Mean and Standard Deviation

A sample histogram(as shown in figure 3) along with its mean value and the standard deviation are also plotted. The histogram is spread over a large range of pixel DN values if the standard deviation is high. The relative shift in the mean and standard deviation help to visualize the change in the gray level distribution of the image bands. The value of the standard deviation is correlated with the possibility to recognize different unities. The statistical control is necessary in order to examine spectral information preservation.

C.3 Process Flow: Microwave Image Classification

Following are the methodological process flow that needs to be followed for classifying microwave satellite images;

- Image variances or speckle is a granular noise that inherently exists in and degrades the quality of the active radar and SAR (Synthetic Aperture Radar) images. Before using active radar and SAR (Synthetic Aperture Radar) imageries, the very first step is to reduce the effect of Speckle noise.
- Speckle filtering consists of moving a kernel over each pixel in the image and applying a mathematical calculation using the pixel values under the kernel and replacing the central pixel with the calculated value. The kernel is moved along the image one pixel at a time until the entire image has been covered. By applying the filter a smoothing effect is achieved and the visual appearance of the speckle is reduced.
- For the purpose of evaluating the performance of the filters quantitatively, two quantities of Mean and Standard Deviation (SD) are used. Based on these two quantities, the best performance filter is selected, if the Mean of filtered image is close to the original image while the Std. Dev. of filtered image has the minimum value.
- Convolution of the image with the filter is to be done so as to get the image in readable form.
- Assigning 0 and 1 values to the pixels whose DN values are greater and lower than the mean respectively.
- Converting the image into black and white image.

III. SOFT COMPUTING USING SVM

Support Vector Machine (SVM) is a supervised classification method derived from statistical learning theory that often yields good classification results from complex and noisy data. The SVM is trained on a set of input ROIs for the image. Output class names, colors, and rule image band names are inherited from the input ROIs. The probable SVM parameters are kernel_type, degree, gamma, bias, penalty, thresh, pyramid_levels, and pyramid_reclass_thresh to control the classification accuracies[15]. These options can also be used to enable the use of hierarchical processing, which provides coarser overall results with reduced processing time. If not specified, the SVM classifier uses ENVI Classic's default SVM options. Support Vector Machine is used to perform supervised classification on images to identify the class associated with each pixel. SVM provides good classification result from complex and noisy data[16][20].

It separates the classes with a decision surface that maximizes the margin between the classes. The surface is often called the optimal hyperplane, and the data points closest to the hyperplane are called support vectors. One can adapt SVM to become a nonlinear classifier through the use of nonlinear kernels. While SVM is a binary classifier in its simplest form, it can function as a multiclass classifier by combining several binary SVM classifiers (creating a binary classifier for each possible pair of classes). ENVI's implementation of SVM uses the pair-wise classification strategy for multiclass classification. SVM classification output is the decision values of each pixel for each class, which are used for probability estimates. The probability values, stored in ENVI as rule images, represent "true" probability in the sense that each probability falls in the range of 0 to 1, and the sum of these values for each pixel equals 1. ENVI performs classification by selecting the highest probability. An optional threshold allows reporting pixels with all probability values less than the threshold as unclassified.

The Support vector machine is a classifier that is derived from statistical learning theory. SVM became famous when, using images as input, it gave accuracy comparable to neural-network with hand-designed features in a handwriting recognition task. Currently, SVM is widely used in object detection & recognition, content-based image retrieval, text recognition, biometrics, speech recognition, etc.

Support vector machines is an algorithm which learns from the examples. For example a SVM machine can detect a handwritten structures by simply undergoing many observations of scanned copies of handwritten papers. An SVM is a recipe for maximizing a particular mathematical function with respect to given collection of data. For understanding the complete working of svm one needs to understand four basic concepts regarding svm (i) the separating hyperplane, (ii) the maximum-margin hyperplane, (iii) the soft margin and (iv) the kernel function[17].

IV. RESULTS AND DISCUSSION

After From results, it is evident that Linear kernel took 0.386 sec, whereas RBF kernel 0.846 sec for training SVM with minimum three basic features of remote sensing images. SVM model parameters are estimated as a outcome of training. Once started learning, the testing time for Linear kernel found to be 28sec and that of RBF is 1132sec[1].

Hyperspectral datasets can be displayed using multispectral data display methods such as RGB composites. Isometric view is another method of displaying hyperspectral data using a 3-D data cube with a color composite on the top. It shows rich information on the sides of the cube. Hyperspectral imagery is typically collected (and represented) as a data cube with spatial information collected in the X-Y plane, and spectral information represented in the Z-direction.

For experimentation, author used Indian Microwave Mission satellite images RISAT, which is acquired in MRS (Moderate Resolution), whereas other type of RISAT images are FRS, HRS, and CRS. The RISAT-1 image of Savner, Nagpur area was captured on 14th Sept, 2013 in MRS mode, from National Remote Sensing Centre (NRSC), Hyderabad. The experimentation performed for both the polarization techniques viz. HH and HV polarization.

When applied Gaussian filter formula on RISAT image having effective spatial resolution of 30m;

$$Gaussian : h = fspecial('gaussian', hsize, sigma);$$

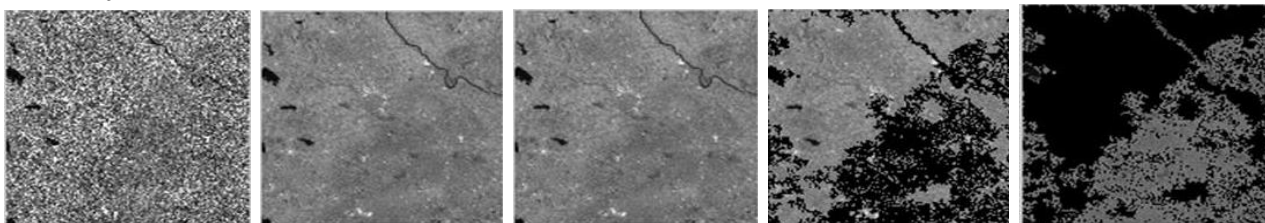
returns a rotationally symmetric Gaussian lowpass filter of size h with standard deviation sigma (positive). H-size can be a vector specifying the number of rows and columns in h, or it can be a scalar, in which case h is a square matrix. The default value for h-size is [3 3]; the default value for sigma is 0.5.

Disk filter can also be applied on same RISAT image, the formula for which is mentioned below;

$$Disk : h = fspecial('disk', radius)$$

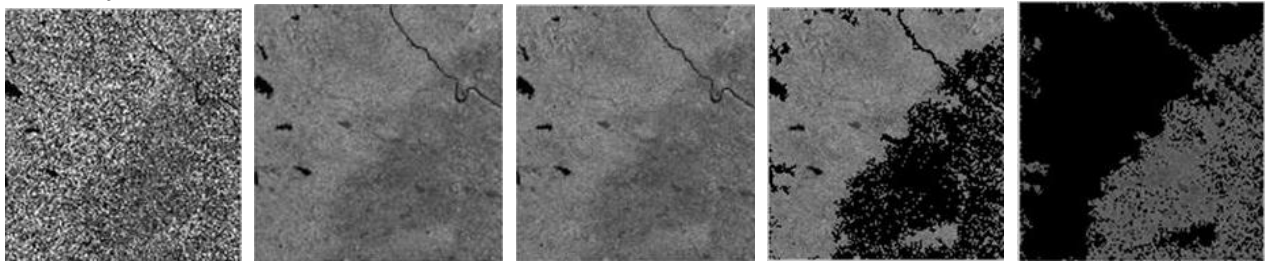
returns a circular averaging filter (pillbox) within the square matrix of size2*radius+1. The default radius is 5. The results for which is shown in following figures.

A. Results for HH (Horizontal-Horizontal) Polarization



(a) Original HH Image (b) Gaussian Filter (c) Disk Filter (d) Non-Agriculture Land (e) Agriculture Land
 Fig.8 Figures showing (a) Original RISAT HH Image (b) Gaussian Filter (c) Disk Filter (d) Non-Agriculture Area (e) Agriculture Land Area

B. Results for HV (Horizontal-Vertical) Polarization



(a) Original HV Image (b) Gaussian Filter (c) Disk Filter (d) Non-Agriculture Land (e) Agriculture Land
 Fig.9 Figures showing (a) Original RISAT HV Image (b) Gaussian HV (c) Disk HV (d) Non-Agriculture Area HV (e) Agriculture Land Area HV

C. Statistical Inference on Area Calculations

Agriculture area estimation is done upon microwave image classification. The statistical figures were generated out of RISAT classified outputs and following inference could be made upon the results so obtained.

TABLE I
 AGRICULTURE AREA ESTIMATION USING RISAT IMAGES

Classified Themes	Type of Polarization Used	
	HH Polarization	HV Polarization
Agricultural land (%)	36.91%	35.66%
Non-agricultural land (%)	63.09%	64.34%

TABLE II
 MEAN & STD. DEVIATION OF POLARISED RISAT IMAGES

Polarization Type	Statistical Inference of RISAT Images	
	Mean	Standard Deviation
Original HH Image	122.290	54.213
Processed HH Image	121.913	20.325
Original HV Image	108.148	58.407
Processed HV Image	107.786	20.283

Following is the graph exhibiting the agriculture acreage estimation in both HH and HV polarization of microwave images by virtue of classification using soft computing.

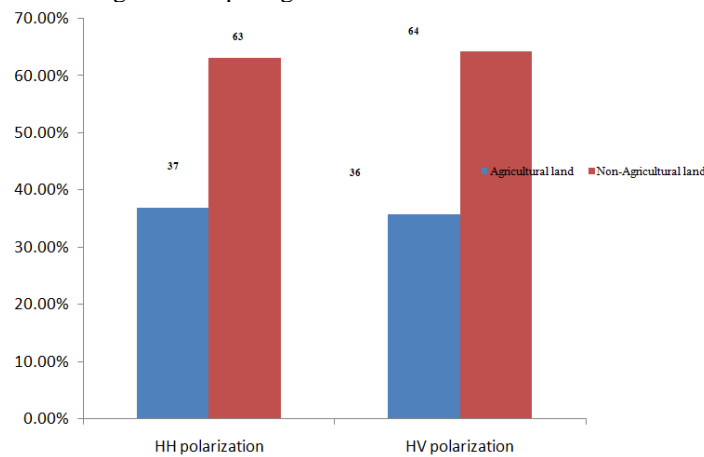


Fig.13 Graph showing agriculture acreage estimation

V. CONCLUSION

Experiments carried out on multi-spectral remote sensing satellite images demonstrated that Linear kernel performs well as compared to RBF Kernel for SVM model training in terms of time. Besides, time taken by Linear Kernel is too less as compared to RBF. The obvious reasons behind may be either data might be quiet linearly separable, and hence RBF might be running the loops unnecessarily and may have been suffered with overfitting problems. Another soft computing approach used 4 kernels of SVM for validating accuracies and time complexity. It was found again Linear Kernel perform well, but at the cost of time. The samples in both cases might be suitably linear and hence other SVM kernels like Polynomial, Sigmoid, RBF, and ANOVA was not performing satisfactorily[4][3].

Recent advances in remote sensing and geographic information has led the way for the development of hyperspectral sensors. Hyperspectral remote sensing, also known as imaging spectroscopy, has wide application range viz. Agricultural, minerals, terrestrial vegetation, plant stress, leaf water content, canopy chemistry, crop type and entire biodiversity spectrum. Minute details are captured in hundreds of spectral bands and hence most useful for crop discrimination. Researchers have taken into consideration spectral profiles obtained from hyperspectral sensors (called as spectral library)

for analyzing and classification of hyperspectral images. The most popular spectral library devised by NASA Jet Propulsion Laboratory (JPL) that uses ASTER satellite data[14].

The studies concluded that the use of optimal parameters would give better classification result in SVM. ENVI was used to find extreme endmembers, which later processed using spectral hourglasses approach. The MNF, PPI and n-D Visualizer methods was used for detailed spectral analysis and it reveals that complex agricultural scenes can be efficiently and accurately classified with hyper-spectral imagery[10].

SAR (Synthetic Aperture Radar) data has the advantage that cannot be influenced by the rain and cloud weather and can penetrate crop in a certain range and the merits make a great contribution to the prevailing trend[7]. From the calculated results, the percentage discrimination obtained is low in HV polarization as compared to HH (Horizontal-Horizontal) polarization, which means that the crop field has the strongest response to horizontal polarization while the weakest response to cross polarization. From the calculated results, it is observed that a good filter has a lower difference between Means of the original and filtered images while preserving a low Standard Deviation for the filtered image which was obtained by using combination of disk and Gaussian filter. The HV polarized form of RISAT microwave satellite image is best suitable for agriculture applications as compared to HH polarization[29]. Future scope lies in data fusion of microwave images with high resolution multi-spectral or hyper-spectral images, so as to get advantages of color and minute bands information, intermingling with the strength of microwave remote sensing technology, day & night coverage, even in cloudy weather of rainy season.

ACKNOWLEDGMENT

The authors wish to thank Director, Maharashtra Remote Sensing Applications Centre, Nagpur for indeed support. Also, we owe our thanks to post graduate research scholar, Ms Priyanka Shewalkar for her inputs on few sections of this research paper. Last but not the least, we would like to express our sincere gratitude to all those who contributed directly or indirectly for making article, a reality.

REFERENCES

- [1] A. Khobragade, P. Athawale and M. Raguwanshi, Optimization of statistical learning algorithm for crop discrimination using remote sensing data," *Advance Computing Conference (IACC), 2015 IEEE International, Bangalore, 2015*, pp. 570-574.
- [2] Anand N. Khobragade, Mukesh M. Raghuvanshi, *Contextual soft classification approaches for crops identification using multi-sensory remote sensing data: Machine learning perspective for satellite images*, Artificial Intelligence Perspectives and Applications, Volume 347 2015, Proceedings of the 4th Computer Science On-line Conference 2015 (CSOC2015), Vol 1: Artificial Intelligence Perspectives and Applications; DOI: 10.1007/978-3-319-18476-0.
- [3] B. Yekkehkhany, A. Safari, S. Homayouni, M. Hasanlou, *A Comparison Study of Different Kernel Functions for SVM-based Classification of Multi-temporal Polarimetry SAR Data, The 1st ISPRS International Conference on Geospatial Information Research*, 15–17 November 2014, Tehran,
- [4] Anand N. Khobragade, Mukesh M. Raghuvanshi, Latesh Malik, "Evaluating Kernel Effect on Performance of SVM Classification using Satellite Images" *International Journal Of Scientific & Engineering Research*, Volume 7, ISSUE 3, March-2016, "Unpublished".
- [5] Mahesh and Mather, 2006; Some issues in the classification of DAIS hyperspectral data, *International Journal of Remote Sensing*, 27 (14). pp. 2895-2916.
- [6] Anand Khobragade, Priyanka Shewalkar, Prof. Kapil Jajulwar, "Review Paper on Crop Area Estimation Using SAR Remote Sensing Data", *IOSR Journal of Electrical and Electronics Engineering (IOSR-JEEE)*, Volume 9, Issue 2 Ver. VII (Mar – Apr. 2014), PP 97-98
- [7] Duin, R.P.W. and Tax, D.M.J., Statistical pattern recognition. In: Chen, C.H., Wang, P.S.P. (Eds.), *Handbook of Pattern Recognition and Computer Vision*, World Scientific Publishing, Singapore. pp. 3-24.
- [8] Xin Niu, and Yifang Ban, "A Novel Contextual Classification Algorithm for Multitemporal Polarimetric SAR Data", *IEEE Geoscience And Remote Sensing Letters*, pp1-5, 2013
- [9] D. G. Hadjimitsis, G. Papadavid, A. Agapiou, K. Themistocleous, M. G. Hadjimitsis, A. Retalis, S. Michaelides, N. Chrysoulakis, L. Toullos, and C. R. I. Clayton "Atmospheric correction for satellite remotely sensed data intended for agricultural applications: impact on vegetation indices" Atmospheric correction for agricultural applications Published by *Copernicus Publications on behalf of the European Geosciences Union*, 2010
- [10] M. Heidari Mozaffar, M. J. Valadan Zoej, M.R. Sahebic, Y. Rezaei "Vegetation endmember extraction in hyperion images" *The International Archives of the Photogrammetry, Remote Sensing and Spatial Information Sciences*. vol. xxxvii. part b7. beijing 2008
- [11] *ENVI user's guide*, FLAASH Module Version 4.3 July, 2006 Edition.
- [12] Prudhvi Gurram, Heesung Kwon, "Contextual SVM For Hyperspectral Classification Using Hilbert Space Embedding", *IEEE, IGARSS 2012*, pp 5470-5473
- [13] H. Kaufmann, K. Segl, S. Itzerott, H. Bach, A. Wagner, J. Hill, B. Heim, K. Oppermann, W. Heldens, E. Stein, A. Müller, S. Van Der Linden, "Hyperspectral Algorithms", *Report in the frame of EnMAP preparation activities Scientific Technical Report STR10/08*
- [14] G. Waldhoff, O. Bubenzer, A. Bolten, W. Koppe, G. Bareth "Spectral analysis of ASTER, hyperion, and quickbird data for geomorphological and geological research in egypt (dakhla oasis, western desert)" *The*

International Archives of the Photogrammetry, Remote Sensing and Spatial Information Sciences. Vol. XXXVII. Part B8. Beijing 2008

- [15] William s Noble “What is a support vector machine?”, *Nature biotechnology*, volume 24 number 12 december 2006.
- [16] Z. Li a, R. Hayward a, J. Zhang A, H. Jin Aa, R. Walker “Evaluation of spectral and texture features for object-based vegetation species classification using support vector machines” In: Wagner W., Székely, B. (eds.): *ISPRS TC VII Symposium – 100 Years ISPRS*, Vienna, Austria, July 5–7, 2010, *IAPRS*, Vol. XXXVIII, Part 7A.
- [17] Anil A. Kumar, V.K. Dadhwal, 2010, “Entropy-based Fuzzy Classification Parameter Optimization using uncertainty variation across Spatial Resolution”, *International Journal of Remote Sensing*, pp179-192,2010
- [18] Kun Li, Yun Shao, Fengli Zhang, “Paddy Rice identification using polarimetric SAR (Synthetic Aperture Radar) data in Southern China”, *IEEE, 2010*.
- [19] DING Yaping, CHEN Zhongxin, “A review of crop identification and area monitoring based on SAR (Synthetic Aperture Radar) image”, China, *2012 IEEE*
- [20] Qiong An, Wanlin Gao, Lina Yu, Jianjia Wu, Bangjie Yang, Wei Liu, “Research on Crop Identification Method Based on Two-Phase Classification Using Remote Sensing in Large Scale”, *China, 2011 IEEE*
- [21] Bai Lina, Wang Bengyu, Tian Xin, Lu Ying, Yang Yongtian, “Winter Wheat Identification Using Multi-Temporal Envisat ASAR Data --A Case Study At Tongzhou District, Beijing”, *IGARSS, 2012*
- [22] Kadim Tasdemir, Selcuk Reis, “Land Cover Identification for Finding Hazelnut Fields Using Worldview-2 Imagery”, *IEEE 2011*
- [23] Qiong An, Wanlin Gao, Bangjie Yang, Jianjia Wu, Lina Yu, Zili Liu, “Research on Feature Selection Method Oriented to Crop Identification Using Remote Sensing Image Classification”, *Sixth International Conference on Fuzzy Systems and Knowledge Discovery, IEEE, 2009*
- [24] L J Han, Y Z Pan , B Jia , X L Zhu,L Xu, S Wang et al “Acquisition of paddy rice coverage based on multi-temporal IRS-P6 satellite AWiFS RS-data”, *Transactions of the CASE*, vol 23,pp. 137-143,2007
- [25] N.D. Herold, “An evaluation of radar texture for land use/cover extraction in varied landscapes,” *International Journal of Applied Earth Observation and Geoinformation*, vol. 5, pp.113–128, 2004.
- [26] T. Le toan, H. Laur, E. Mougin, A. Lopes, “Multitemporal and Dual-Polarization Observations of Agricultural Vegetation Covers by X-Band Sar Images,” *IEEE Transactions on Geoscience and Remote Sensing*, New York, vol. 27, No.6, pp. 709-718, November 1989.
- [27] Y. Shao et al., “Rice monitoring and production estimation using multitemporal RADARSAT,” *Remote Sensing of Environment*, New York, vol.76, No.3, pp. 310-325, June 2001.
- [28] *Tutorial: Fundamentals of Remote Sensing*: <http://www.nrcan.gc.ca/earth-sciences/geomatics/satellite-imagery-air-photos/satellite-imagery-products/educational-resources/9309>
- [29] Ahmed A. Mostafa, Christian Debes, Abdelhak M. Zoubir, "Segmentation by Classification for Through-the-Wall Radar Imaging Using Polarization Signatures", *IEEE Transactions On Geoscience And Remote Sensing*, vol. 50, no. 9, september 2012, pp 3425-3439
- [30] Lien Loosvelt, Jan Peters, Henning Skriver, Bernard De Baets, and Niko E. C. Verhoest, "Impact of Reducing Polarimetric SAR Input on the Uncertainty of Crop Classifications Based on the Random Forests Algorithm", *IEEE Transactions On Geoscience And Remote Sensing*, vol. 50, no. 10, october 2012, pp 4185-4200
- [31] Solberg, A.H.S.; Jain, A.K.; Taxt, T., 2002, Multisource classification of remotely sensed data: fusion of Landsat TM and SAR images, *IEEE transactions on Geoscience and Remote Sensing*, vol. 32,issue: 4, abstract